

Monte Carlo Variational Transition-State Theory Study of the Unimolecular Dissociation of RDX

Dmitrii V. Shalashilin[†] and Donald L. Thompson*

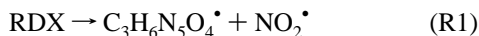
Department of Chemistry, Oklahoma State University, Stillwater, Oklahoma 74078

Received: June 13, 1996; In Final Form: July 30, 1996[⊗]

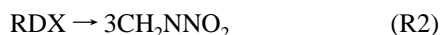
Monte Carlo variational transition-state theory (MCVTST) has been used to calculate unimolecular dissociation rates for RDX (hexahydro-1,3,6-trinitro-1,3,5-triazine) for total energies over the range 170–450 kcal/mol. The calculations were done using the potential energy surface (PES) developed by Chambers and Thompson (*J. Phys. Chem.* **1996**, *99*, 15881). This PES allows for dissociation to occur by bond fission (energy required: 48 kcal/mol) and by concerted triple bond fission (energy barrier: 37 kcal/mol); these are the dominant primary dissociation channels consistent with the results of the molecular beam infrared multiphoton dissociation (MB-IRMPD) experiments of Zhao, Hints, and Lee (*J. Chem. Phys.* **1988**, *88*, 801). The computed branching ratio for ring to simple bond fission at 170 kcal/mol is in good agreement with the value (~ 2) determined from the MB-IRMPD data. The rates for the two reaction channels and the ratio of the rates are compared to classical trajectory results; the agreement is good, as expected, at the lower energies, but diverges after the total energy exceeds about 250 kcal/mol. However, the ratio of the rates is comparable for the entire energy range. We find that the TST dividing surface for the concerted molecular elimination (i.e., ring fission) is correlated with the ring opening, the initial stage of the reaction, thus simplifying the definition of the surface dividing reactants and products defined by the minimum flux. We also show how importance sampling can be used to facilitate the computations.

I. Introduction

The initial decomposition reactions of RDX (hexahydro-1,3,6-trinitro-1,3,5-triazine) (see Figure 1) apparently depend on the experimental conditions, particularly the physical state.¹ However, the elimination of NO₂ by simple rupture of one of the three N–N bonds,



is observed for all conditions. Molecular beam infrared multiphoton dissociation (MB-IRMPD) experiments² show that decomposition of gas-phase RDX also occurs by ring (triple C–N bond) fission,



and that this reaction is competitive with (R1); the experimentally determined ratio of concerted molecular elimination (R2) to simple N–N bond fission (R1) is about 2. However, reaction R2 has not been observed in condensed-phase systems.

We have reported a series of classical trajectory studies that were done in an effort to develop a potential energy surface (PES) and to understand the fundamental dynamics,³ conformational changes,^{4,5} and unimolecular reactions^{6,7} of RDX. Both the formulation of an accurate potential energy surface (PES) and the dynamics calculations are challenging problems because of the size and complexity of the system. The molecule is too large for extensive *ab initio* quantum chemistry calculations to determine a global PES that describes the decomposition reactions. Thus, we have made use of the limited spectroscopic, thermodynamic, and kinetic data to construct an “empirical” PES. While the energy required for the N–N bond rupture reaction (R1) is reasonably well-established (to within a few

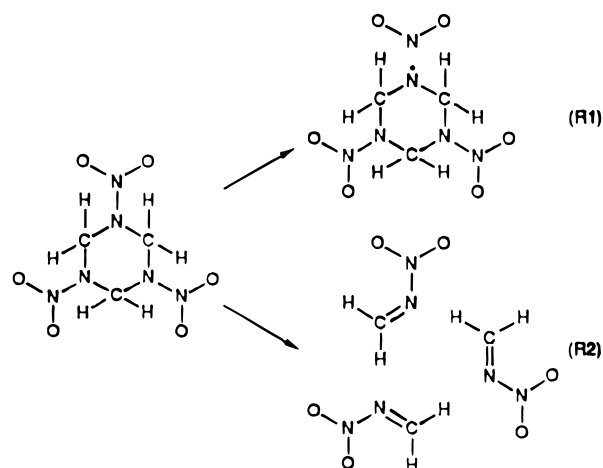


Figure 1. RDX (hexahydro-1,3,6-trinitro-1,3,5-triazine) and the MB-IRMPD products.

kilocalories per mole), there is some uncertainty about the energy barrier for the ring fission reaction (R2). Some *ab initio* results indicate that it is on the order of 70 kcal/mol;⁸ however, our calculations^{6,7} suggest that the barrier must be less than 40 kcal/mol in order to obtain results in accord with the MB-IRMPD experiments.²

We have assumed that the MB-IRMPD results provide a critical test of the PES, and thus we have focused on comparisons of the computed results to the measured branching ratio and product energy distributions reported by Zhao *et al.*² The estimated total energy at which dissociation occurs in these experiments is in the range 150–170 kcal/mol. It is not feasible to perform trajectory calculations at these energies because of the long integration times that are required for reactions to occur. Thus, the dynamics calculations have been for relatively high energies (≥ 200 kcal/mol), and the comparisons are based on extrapolations down to the experimental energies. As we have

[†] On leave from the Institute of Chemical Physics, Russian Academy of Science, 117334 Moscow, Russian Federation.

[⊗] Abstract published in *Advance ACS Abstracts*, December 15, 1996.

recently illustrated, there are dynamics effects at such high energies that make it difficult to do simple extrapolations.⁹

Unimolecular rates are limited by the rate of intramolecular vibrational energy transfer (IVR) at high energies. However, the dynamics at energies near threshold often behave statistically. In the statistical regime, the unimolecular rate constants can usually be represented by simple theories such as RRK. The RRK equation is

$$k(E) = \nu \left(1 - \frac{E^*}{E}\right)^{s-1} \quad (1)$$

where ν is a frequency factor, E^* is the energy required for reaction, and s is the number of effective degrees of freedom. Since trajectory calculations are usually performed for energies well in excess of the statistical regime, fits of eq 1 to the computed rates often result in values of s which are significantly lower than $3N - 6$ (see Table I of ref 9). In ref 9, we examined the statistical and nonstatistical behavior of simple bond rupture in a relatively large molecule (dimethylnitramine) over a range of energies extending from the reaction threshold region up to a few hundred kilocalories per mole above it. In that study, we used classical trajectories and Monte Carlo variational transition-state theory (MCVTST) calculations^{10,11} to calculate rates and analyzed them in terms of RRK theory and IVR rates.

The advantage of MCVTST is that the statistical rates can be calculated for general potential energy surfaces, e.g., one used in a classical trajectory simulation. It is not necessary to make simplifying assumptions such as separability or harmonicity for the molecular modes. The MCVTST rates can be accurately fit by eq 1 with $s = 3N - 6$; however, it is necessary to do the MCVTST calculations in order to determine the frequency factor ν . Thus, it is necessary to use a combination of MCVTST and classical trajectory calculations in order to describe the reaction over a wide energy range.

In the present study, we have used MCVTST to calculate the rates of unimolecular decomposition of RDX. The calculations span the range of energies from the experiment² (170 kcal/mol) to the energies of the classical trajectory studies^{6,7} (200–450 kcal/mol). The result at 170 kcal/mol is in good agreement with the experimental result of Zhao *et al.*² Comparisons of the MCVTST rates for the higher energies to the trajectory results illustrate the extent of the dynamical effects.

It is necessary to make some approximations for a system of this size. The main approximations here are that the dynamics are classical and those involved in the construction of the potential energy surface. Thus, the results could be affected if quantization effects are not negligible. However, it is not easy to ascertain this without making other assumptions which could be questionable. For example, RRKM calculations could be used to introduce quantization, but it is necessary to assume separable, harmonic vibrational modes for the system. We believe that neglecting quantization is often a much less severe approximation than those. The other important approximations in the model used here are those used in formulating the potential. Those, however, are the ones we wish to evaluate by making the comparison with the MB-IRMPD experiment.²

This study also illustrates how the MCVTST approach can be used to study complex reactions for conditions near reaction thresholds where the statistical approximation is usually valid and where it is usually not possible to use classical trajectory simulations. We also show how to use importance sampling in MCVTST to facilitate calculations of microcanonical rate coefficients for large molecules.

II. Theory and Computational Methods

Transition-State Theory. In transition-state theory the microcanonical rate constant is determined by the flux through

a dividing surface S^*

$$k^{\text{TST}}(E) = k^{\text{statistical}}(E) = \frac{\int_{S^*} \delta(H(p,q) - E) v_{\perp} dS^*}{\int_V \delta(H(p,q) - E) d\Gamma} \quad (2)$$

where S^* is theoretically a hypersurface, which depends on all of the phase-space variables, that separates reactants and products and v_{\perp} is the velocity at S^* perpendicular to S^* in the direction of products. The integral in the numerator is over the transition-state region, and the one in the denominator is over all of the phase space of the reactant.

For simple bond fission eq 2 can be written as

$$k^{\text{TST}}(E) = \frac{1}{2} \frac{\int_V \delta(H(p,q) - E) \delta(r - r^*) |\dot{r}| d\Gamma}{\int_V \delta(H(p,q) - E) d\Gamma} \quad (3)$$

Further simplification can be achieved since the integration over momentum space can be done analytically, which gives

$$k^{\text{TST}}(E) = \frac{1}{2} \frac{\int_{V^c} W(\mathbf{q}) \langle |\dot{r}_{\text{RC}}| \rangle \delta(r_{\text{RC}} - r^*) d\mathbf{q}}{\int_{V^c} W(\mathbf{q}) d\mathbf{q}} \quad (4)$$

where¹²

$$W(\mathbf{q}) = [E - V(\mathbf{q})]^{(3N-5)/2} \quad (5)$$

$$\langle |\dot{r}_{\text{RC}}| \rangle = (4(E - V(q)) / (3\pi(N - 1)\mu_r))^{1/2} \quad (6)$$

V^c indicates that the integrals are over only the configuration space; $\mu_r = \mu_i \mu_j / (\mu_i + \mu_j)$, the reduced mass of the two atoms making up the breaking bond. This method is obviously more efficient numerically, because one has to integrate over $3N$ -dimensional configuration space $V^c \{d\mathbf{q}\}$ instead of $6N$ -dimensional phase space $V \{d\Gamma = d\mathbf{p} d\mathbf{p}\}$. Integration over Cartesian momentum space^{11h} was performed to obtain eqs 4–6 by exploiting the fact that the kinetic energy is diagonal in Cartesian coordinates.

We carefully checked the agreement of results for eqs 3 and 4. We had done so earlier also.⁹ We used the agreement between the two to test the computer code.

Monte Carlo Sampling. A convenient way to estimate the integrals in eqs 3 and 4 is to use Metropolis Monte Carlo sampling,¹³ which is an efficient method for evaluating multi-dimensional integrals of the type

$$\langle g \rangle = \frac{\int_V f(\Gamma) g(\Gamma) d\Gamma}{\int_V f(\Gamma) d\Gamma} \quad (7)$$

In the Metropolis method the function $f(\Gamma)$ determines the probability of accepting an attempted random move $\Gamma_i \rightarrow \Gamma_{i+1}$. Each time there is an attempt to move the system to a new configuration a new value of $f(\Gamma)$ is calculated. If $f(\Gamma_{\text{new}}) > f(\Gamma_{\text{old}})$, the move is accepted and $\Gamma_{i+1} = \Gamma_{\text{new}}$. If $f(\Gamma_{\text{new}}) < f(\Gamma_{\text{old}})$, the move is accepted with probability $f(\Gamma_{\text{new}})/f(\Gamma_{\text{old}})$; otherwise the move is rejected, and $\Gamma_{i+1} = \Gamma_{\text{old}} = \Gamma_i$. Integrals of the kind in eq 7 (i.e., those in eqs 3 and 4) can be estimated by

$$\langle g \rangle = \frac{\sum_{i=1, N} g(\Gamma_i)}{N} \quad (8)$$

where N is a large number.¹³

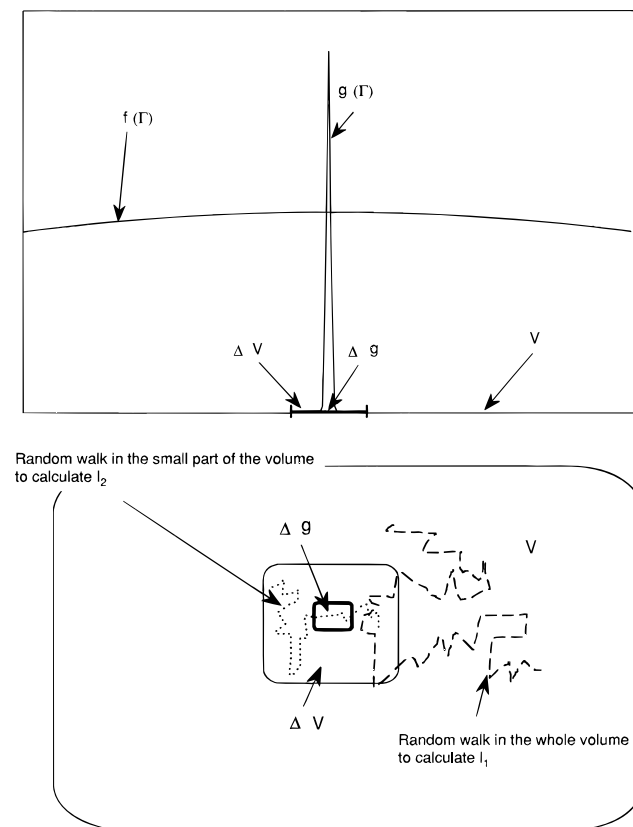


Figure 2. Upper frame: Illustration of a narrow function in the volume V and the auxiliary volume ΔV . Lower frame: Illustration of a random walk in V for the calculation of integral I_1 and a random walk in ΔV to calculate the integrals I_2 (see eq 9).

In practice it is necessary to replace the δ functions in eqs 3 and 4 by a narrow function; here we used a step function: $\delta(x) \cong h = 1/2\epsilon$, if $|x| < \epsilon$; $\delta(x) \cong h = 0$, otherwise. The maximum step sizes in the Markov walks were such that the acceptance/rejection ratio fell in the range 0.3–0.8.

We used importance sampling¹⁰ to speed up the convergence of the sum eq 8. This is effective when g in eq 7 is a narrow function and only a small part Δg of the integration space contributes to the integral (which is the case here), as illustrated in Figure 2. The random walk visits the region Δg very infrequently, which results in very slow convergence of the sum in eq 6. To speed up the convergence, one can choose a part ΔV of the integration space V such that $\Delta g \ll \Delta V \ll V$ and $\Delta g \in \Delta V$. Then, eq 7 can be rewritten as

$$\begin{aligned} \langle g \rangle &= \frac{\int_V f(\Gamma) g(\Gamma) d\Gamma}{\int_V f(\Gamma) d\Gamma} \\ &= \frac{\int_{\Delta V} f(\Gamma) d\Gamma}{\int_V f(\Gamma) d\Gamma} \frac{\int_{\Delta V} f(\Gamma) g(\Gamma) d\Gamma}{\int_{\Delta V} f(\Gamma) d\Gamma} \\ &= \frac{\int_V G(\Gamma) f(\Gamma) d\Gamma}{\int_V f(\Gamma) d\Gamma} \frac{\int_{\Delta V} f(\Gamma) g(\Gamma) d\Gamma}{\int_{\Delta V} f(\Gamma) d\Gamma} = I_1 I_2 \quad (9) \end{aligned}$$

where G is an auxiliary biasing function

$$G(\Gamma) = \begin{cases} 1 & \Gamma \in \Delta V \\ 0 & \Gamma \notin \Delta V \end{cases} \quad (10)$$

If $g(\Gamma) = 0$ for $\Gamma \notin \Delta V$, then eq 9 is exact. Convergence

of the two integrals in eq 9 requires many fewer steps in the Metropolis walk than in the direct calculation of the integrals in eq 5. If $f(\Gamma)$ is a smooth function (e.g., a constant), the number of steps N in a direct calculation of the integrals in eq 7 is inversely proportional to the ratio of the volume which contributes to the integral and the total volume:

$$N' \propto V/\Delta g \quad (11)$$

Similarly, if eq 9 is used, the number of steps for calculating the two integrals I_1 and I_2 is

$$N \propto \frac{V}{\Delta V} + \frac{\Delta V}{\Delta g} \quad (12)$$

and the ratio is

$$\frac{N}{N'} = \frac{\Delta g}{\Delta V} + \frac{\Delta V}{V} \ll 1 \quad (13)$$

It is a minimum when $\Delta V = [\Delta g V]^{1/2}$.

We used importance sampling for calculations at energies less than 200 kcal/mol, where standard sampling converges extremely slowly. The volume ΔV and auxiliary function were determined by the condition

$$G = \begin{cases} 1 & \text{if } 2.0 \text{ \AA} < r_{C-N} < 2.6 \text{ \AA} \\ 0 & \text{otherwise} \end{cases} \quad (14)$$

for the bond rupture reaction (R1) and

$$G = \begin{cases} 1 & \text{if } 1.9 \text{ \AA} < r_{N-N} < 2.1 \text{ \AA} \\ 0 & \text{otherwise} \end{cases} \quad (15)$$

for the ring opening reaction (R2).

The volume Δg is determined by the width ϵ of the δ -function

$$\delta(r - r_0) \cong \begin{cases} 1/2\epsilon & \text{if } |r - r_0| < \epsilon \\ 0 & \text{if } |r - r_0| > \epsilon \end{cases} \quad (16)$$

The values of ϵ were taken to be 0.05 Å for N–N bond fission (R1) and 0.02 Å for ring opening (R2). The location of the dividing surface (i.e., r_0) was determined variationally corresponding to the minimum value of the rate constant. We made sure that (using a Taylor's series expansion)

$$(d^2k(r_0)/dr_0^2) \frac{\epsilon^2}{k(r_0)^2} \ll 1 \quad (17)$$

near the minimum $r_0 = r_0^{\min}$, that is, that ϵ is sufficiently small that the calculated rate is unaffected by it.

The rates of convergence of the calculations with importance sampling were at least an order of magnitude faster than those done without it. In fact, importance sampling makes the calculations feasible. For example, the rates at energies lower than 200 kcal/mol did not converge for 2×10^8 steps when the Markov walk was over the entire configuration space (i.e., direct evaluation of eq 4); however, when importance sampling was used, the integrals

$$I_1 = \frac{\int_{\Delta V^c} W(\mathbf{q}) d\mathbf{q}}{\int_{V^c} W(\mathbf{q}) d\mathbf{q}} = \frac{\int_{V^c} G W(\mathbf{q}) d\mathbf{q}}{\int_{V^c} W(\mathbf{q}) d\mathbf{q}} \quad (18)$$

$$I_2 = \frac{\int_{\Delta V^c} W(\mathbf{q}) \langle |\dot{r}_{RC}| \rangle \delta(r_{RC} - r^*) d\mathbf{q}}{\int_{\Delta V^c} W(\mathbf{q}) d\mathbf{q}} \quad (19)$$

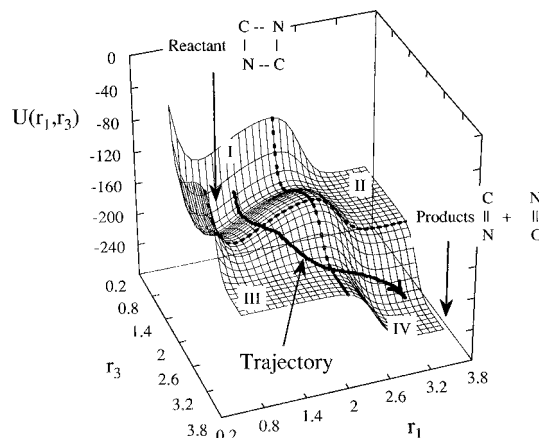


Figure 3. Ring fission molecular elimination reaction of RDX occurs when one of the C–N bonds breaks. This is accompanied by formation of double bonds in the adjacent C–N bonds and weakening (and subsequent breaking) of the alternate C–N bonds around the ring. This process is illustrated here with a model PES for a simple four-membered ring (see eq 21). The illustration is for a dimer, while RDX is a trimer. The model was designed for clarity, not accuracy (e.g., the reaction enthalpy is qualitatively different in the model and in RDX).

converged to within 10% accuracy after 2×10^7 and 5×10^6 steps, respectively.

Dividing Surfaces. Strictly speaking, the dividing surface S^* is a function of all of the coordinates and momenta, but in practice S^* can usually be defined by only a few coordinates. For simple bond-rupture reactions, the dividing surface can be defined as a function of the internuclear separation r^* of the pair of atoms for the bond (N–N in the present case). Rigorously, the value of r^* should be chosen so that the flux through the dividing surface is minimized.

Since there are three NO_2 groups in RDX, the total rate constant for simple bond rupture (SBR) is

$$k_{\text{SBR}} = 3k_{\text{N-N}} \quad (20)$$

For a concerted reaction the choice of S^* is more complex. It is usually necessary to define it in terms of several coordinates. For the present case, because of the nature of the potential,^{6,7} which is based on the idea of concerted ring decomposition into three units of CH_2NNO_2 , it is possible to use a somewhat simplified dividing surface. The potential is formulated such that when one of the ring C–N bonds breaks, the two alternate C–N weaken and the three other C–N bonds become stronger (i.e., double bonds form). This is accomplished with switching functions.^{6,7}

Since the RDX PES is rather complicated, it is instructive to consider a simpler example. The RDX molecule is a trimer of CH_2NNO_2 ; however, we can illustrate the concerted ring fission by considering a dimer. Each unit of the dimer is denoted by C–N (for the illustration we can consider only the ring atoms); that is, we consider the model reaction



A plot of the surface $V(r_1, r_3)$ for this reaction is shown in Figure 3; the simple model PES was obtained by using some modifications of the PES parameters given in ref 7. All of the bending interactions are neglected, and it is assumed that $r_2 = r_4 = a$ constant. Four regions I, II, III, and IV are labeled in Figure 3. Region I corresponds to the reactant $(\text{CN})_2$, region IV corresponds to separated products $\text{CN} + \text{CN}$, and regions II and III are the regions where the ring is open but only one of the bonds has been broken. To go from region I to region IV, a trajectory

TABLE 1: Ring Bond Fissions as a Function of Time^a

$t/\Delta t$	N_1	N_3	N_5	N_{135}	N_2	N_4	N_6	N_{246}
1	2	2	2	2	4	3	3	3
2	3	3	3	3	5	5	5	5
3	5	5	5	5	5	5	5	5
4					5	5	5	5
5	5	5	5	5	5	5	5	5
6	5	5	5	5	5	5	5	5
7	7	7	9	7	5	5	5	5
8	10	10	10	10	5	6	6	5
9	11	11	11	11	7	7	7	7
10	11	11	11	11	7	7	7	7
11	11	11	11	11	7	7	7	7
12	11	11	11	11	8	8	8	8
13	12	12	12	12	10	10	10	10
14	12	12	12	12	10	10	10	10
15	12	13	12	12	10	10	10	10
16	13	13	13	13	10	11	10	10
17	14	15	15	14	11	11	11	11
18	15	16	16	15	11	11	11	11
19	17	17	17	17	11	11	11	11

^a The number of trajectories N_i in which one of the six C–N ring bonds had ruptured and the number of trajectories N^{CME} in which three of the C–N broke are given at intervals of time $n = t/\Delta t$ ($\Delta t = 2.6 \times 10^{-14}$ s). In some cases there was an initial C–N bond fission but no subsequent bond fissions to give complete decomposition; these are indicated by bold type. The subscripts, 1, 2, ..., 6 indicate a numbering of the rings bonds. The total energy is 400 kcal/mol.

must cross two ridges (marked by dashed lines), corresponding to the rupture of bonds r_1 and r_3 . Crossing the ridge between I and II or between I and III corresponds to the ring opening by rupture of one of the ring bonds. Subsequent crossing of the ridge between regions II and IV or that between regions III and IV leads to the product valley. The heights of the second ridges (those between II and IV and between III and IV) are much lower than the ridges for the initial ring opening bond rupture. Thus, the initial bond rupture is the bottleneck in the concerted molecular elimination. After a trajectory has crossed the first ridge, the crossing of the second one follows very quickly.

Thus, the dividing surface in the MCVTST calculation can be defined by using the variables associated with the first ridge. To verify this we performed some trajectory calculations for RDX using the Chambers–Thompson⁷ PES. The initial conditions for the trajectories were selected by using the same Monte Carlo procedure as described above for the MCVTST calculations. We used the trajectories to determine the correlation between the rates of initial ring opening and concerted reaction. Table 1 shows the number of trajectories for which the ring opens and then the concerted reaction occurs. As in ref 7, the initial conditions for an ensemble of 200 trajectories were picked randomly and then we determined the number of trajectories for which one of the ring bonds broke (ring opening) and for which three alternate C–N bonds broke (complete depolymerization). Though there are some differences (shown in bold font), there is good correlation between the two. This confirms that the rupture of one of the bonds is very quickly followed by the rupture of two others.

Thus, the MCVTST rate constant calculation for the concerted reaction is simplified. To determine the rate of the concerted reaction, we can simply calculate the rate of the initial bond rupture that opens the ring. The rate of concerted molecular reaction (CME) can be expressed as

$$k_{\text{CME}} = k_{1,3,5} + k_{2,4,6} = 2k_{\text{CN}} \quad (22)$$

where we identify the alternate sets of CN bonds as 1, 3, 5 and 2, 4, 5.

The dividing surface for each reaction was determined by calculating the flux for a series of 10 surfaces. The flux was

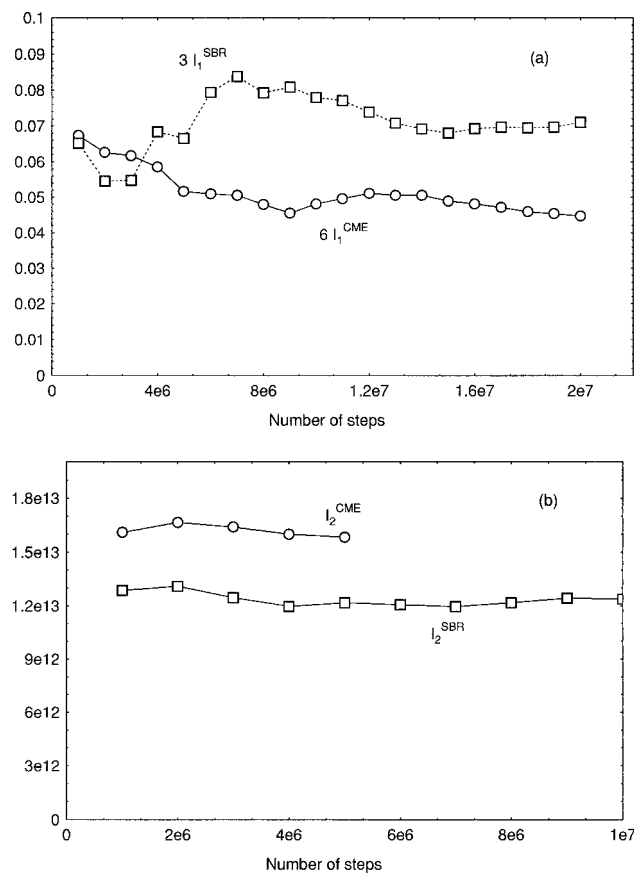


Figure 4. Plots of integrals I_1 and I_2 (see eqs 9, 18, and 19) as functions of the number of steps (where $4e6$, for example, means 4×10^6) in the Markov walk. Circles correspond to N–N bond fission which subsequently leads to concerted molecular elimination (CME), and squares correspond to N–N bond rupture (SBR). The rate constants of individual bond ruptures are $k_{NN} = I_1^{NN} I_2^{NN}$ and $k_{CN} = I_1^{CN} I_2^{CN}$. The rates of reactions R1 and R2 are $k_{SBR} = 3k_{NN}$ and $k_{CME} = 2k_{CN}$. These results are for $E = 300$ kcal/mol.

calculated for dividing surfaces located at 10 values of r_{NN} over the interval $2.1\text{--}3 \text{ \AA}$ for the simple bond rupture reaction and 10 values of r_{CN} over the interval $1.9\text{--}2.1 \text{ \AA}$ for the ring fission reaction. The minimum of k_{NN} was found to be at $r_{NN} = 2.55 \text{ \AA}$, and the minimum of k_{CN} was found at $r_{CN} = 2.0\text{--}2.1 \text{ \AA}$ (depending on the energy). There is less variation in k_{NN} as a function of the location of the dividing surface than in the case of k_{CN} .

The rates of convergence of the Monte Carlo averages are shown in Figure 4 for $E = 300$ kcal/mol. Parts a and b of Figure 4 show plots of the integrals I_1 and I_2 (see eq 9) as functions of the number of Markov steps for ring fission (circles) and simple bond rupture (squares), respectively. Since these reactions can occur, respectively, in six and three different ways, we also checked the convergence of the results by comparing the rates for these identical channels; the variations in these results give estimates of the Monte Carlo error of about 10–15%.

III. Results and Discussion

The MCVTST calculated rates are given (squares) in Figure 5; the results for simple N–N bond rupture are shown in the upper frame of Figure 5 and those for the ring fission reaction in the lower frame. The rates are plotted according to the RRK energy dependence, that is, $\log k$ versus $\log(1 - E^*/E)$; the straight lines in the plots are fits of the MCVTST rates to the RRK equation

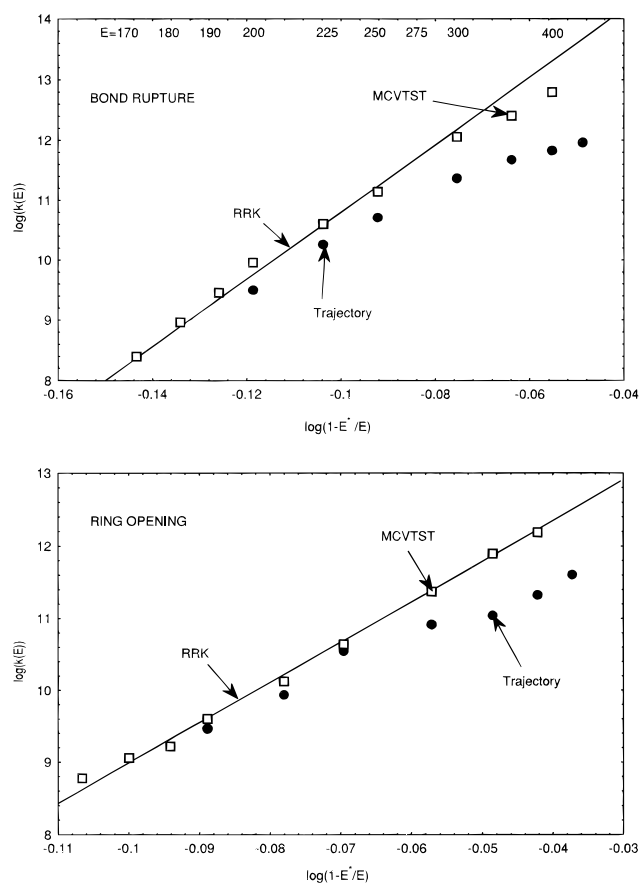


Figure 5. MCVTST rate constants for N–N bond fission (upper frame) and concerted molecular elimination (lower frame), shown as squares. The classical trajectory results from ref 7 are shown as circles, and RRK theory fit to the MCVTST points is shown by the solid line.

$$k(E) = \nu \left(1 - \frac{E^*}{E}\right)^{s-1} \quad (23)$$

The classical trajectory results reported by Chambers and Thompson⁷ are shown as circles.

There is good agreement between the MCVTST and classical trajectory results for both N–N bond rupture and ring fission for energies in the range 200–250 kcal/mol, although the statistical rates are greater than the dynamical rates for the entire energy range studied. The two calculations give the same energy dependence at the lower energies; however, at higher energies the trajectory rates are much less strongly dependent on the energy than are the statistical rates. The classical trajectory results are not well-described by RRK theory over the entire range of energies, although at the lower energies (see Figure 4) the dynamics results begin to behave statistically. This is typical for unimolecular dissociation.¹¹ We have recently addressed this point in a study of a model polyatomic molecule.⁹ We have shown in ref 9 that this behavior is due to the competition between chemical reaction and intramolecular vibrational energy exchange.

The MCVTST results are well-described by the simple RRK theory, eq 23. The solid lines in Figure 5 are plots of the RRK equation fit to the calculated results. In each case, we assumed that E^* is equal to the static potential barrier and then determined the values of ν and s by linear least-squares fitting. The calculated value of s for both reaction channels is 57; that is, it has the expected theoretical value of $3N - 6$. This is not surprising since even for total energies in the region just above 170 kcal/mol the average energy per mode is low relative to the dissociation energy; thus, the harmonic approximation should be valid. The MCVTST calculation also yields a value of the

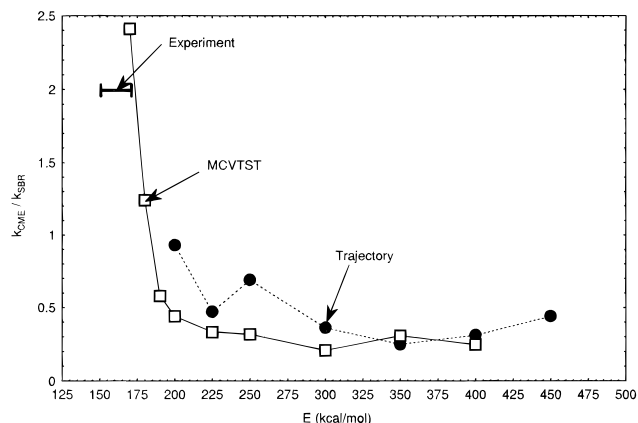


Figure 6. Computed branching ratio $k_{\text{CME}}/k_{\text{SBR}}$. The MCVTST and classical trajectory (ref 7) values are shown as squares and circles, respectively. The horizontal bar is the experimental branching ratio reported by Zhao *et al.*²

frequency factor ν , which depends on the parameters of the transition state, in a relatively simple and straightforward way. In ref 9, we give a detailed discussion of the correspondence between trajectory simulations, MCVTST, and RRK theory.

Figure 6 shows plots of the branching ratio $k_{\text{SBR}}(E)/k_{\text{CME}}(E)$ as a function of energy calculated by using MCVTST (squares) and classical trajectories⁷ (circles); the experimental value² of 2 for the branching ratio is shown as a horizontal bar since there is some uncertainty in the total energy of the molecule when it dissociates.

The estimated total excitation of the molecule upon dissociation in the MB-IRMPD² experiments was estimated to be 80–90 kcal/mol above the zero-point energy (80 kcal/mol), giving a total energy $E_{\text{total}} = E_{\text{excitation}} + E_{\text{zpe}} \approx 160\text{--}170$ kcal/mol. This is the total energy we used in the classical trajectory and MCVTST calculations. Our calculation is in relatively good agreement with the experimental branching ratio of 2. Better agreement with experiment might be obtained for a slightly higher barrier to the ring fission reaction. Nevertheless, the present PES surface appears to be approximately correct.

Some recent experiments^{14–16} on the decomposition of condensed-phase RDX are relevant here. The ring fission reaction is not observed in these experiments. This is likely due to the differences in the experimental conditions in refs 14–16 and those in the MB-IRMPD experiments.² The estimated temperature of the RDX condensed-phase experiment^{14–16} is ~ 1000 K, which gives a total energy $E_{\text{total}} = skT + E_{\text{zpe}} = 57kT + E_{\text{zpe}} \approx 190\text{--}200$ kcal/mol. At this energy the branching ratio is much less than 2; however, our calculations show that the concerted ring fission reaction is still significant. The estimation of experimental temperature is rough, and if the temperature is higher than assumed, the N–N bond fission might be dominant. However, we believe that the explanation for the differences between the gas- and condensed-phase results is due not only to the differences in temperatures (energies) in the experiments but also due to condensed-phase effects such as Wight and Botcher¹⁵ have suggested; they pointed out that the “volume of activation” might dampen the ring fission reaction in solids and liquids—the surrounding molecules simply inhibit this decomposition path.

IV. Summary and Conclusions

We have used Monte Carlo variational transition-state theory (MCVTST) to compute unimolecular dissociation rate coef-

ficients for RDX (hexahydro-1,3,6-trinitro-1,3,5-triazine). The calculations are for total energies over the range 170–450 kcal/mol, thus spanning the range from the experimental energies for the molecular beam IRMPD experiments of Zhao *et al.*² and our previous studies using classical trajectories.^{6,7} The potential energy surface used in the present calculations is the one reported previously.⁷ This PES allows RDX to dissociate by bond fissions (the N–N bonds are the weakest, requiring 48 kcal/mol to break) and by concerted molecular elimination involving the rupture of three C–N bonds in the ring (37 kcal/mol is required to break the first ring bond).

The computed branching ratio (ring fission to simple bond rupture) at 170 kcal/mol is in good agreement with the value of 2 measured by Zhao *et al.*² Furthermore, the computed statistical rates are in good agreement with the previously reported classical trajectory results^{6,7} at the lower energies but diverge for energies in excess of about 250 kcal/mol, although the ratio of the rates are comparable over the entire energy range studied. There are significant dynamical effects due to the limiting IVR rates at the higher energies, thus causing the differences in the trajectory and MCVTST rates. The simple RRK equation can be accurately fit to the MCVTST rates, although RRK theory cannot be used to predict the rates since the frequency factor must be determined by other means (such as MCVTST).

This study shows that the PES⁷ “predicts” the measured reaction-branching ratio. Furthermore, we have illustrate how the MCVTST approach can be used to efficiently compute unimolecular rates for large, complex molecules.

Acknowledgment. This work was supported by the U.S. Army Research Office.

References and Notes

- (1) See, for example: Adams, G. F.; Shaw, R. W., Jr. *Annu. Rev. Phys. Chem.* **1992**, *43*, 311.
- (2) Zhao, X.; Hints, E. J.; Lee, Y. T. *J. Chem. Phys.* **1988**, *88*, 801.
- (3) Sewell, T. D.; Chambers, C. C.; Thompson, D. L.; Levine, R. D. *Chem. Phys. Lett.* **1993**, *208*, 125.
- (4) Wallis, E. P.; Thompson, D. L. *Chem. Phys. Lett.* **1992**, *189*, 363.
- (5) Wallis, E. P.; Thompson, D. L. *J. Chem. Phys.* **1993**, *99*, 2661.
- (6) Sewell, T. D.; Thompson, D. L. *J. Phys. Chem.* **1991**, *95*, 6228.
- (7) Chambers, C. C.; Thompson, D. L. *J. Phys. Chem.* **1995**, *99*, 15881.
- (8) Habibollahzadeh, D.; Grodzicki, M.; Seminario, J. M.; Politzer, P. *J. Phys. Chem.* **1991**, *95*, 7699.
- (9) Shalashilin, D. V.; Thompson, D. L. *J. Chem. Phys.* **1995**, *105*, 1833.
- (10) Doll, J. D. *J. Chem. Phys.* **1980**, *73*, 2769; **1981**, *74*, 1074.
- (11) For some applications of MCVTST see: (a) Viswanathan, R.; Raff, L. M.; Thompson, D. L. *J. Chem. Phys.* **1984**, *81*, 828; **1984**, *81*, 3118. (b) Voter, A. F.; Doll, J. D. *J. Chem. Phys.* **1984**, *80*, 5814; **1984**, *80*, 5832; **1985**, *82*, 80. (c) Voter, A. F. *J. Chem. Phys.* **1985**, *82*, 1890. (d) Raff, L. M.; NoorBatcha, I.; Thompson, D. L. *J. Chem. Phys.* **1986**, *85*, 3081. (e) Rice, B. M.; Raff, L. M.; Thompson, D. L. *J. Chem. Phys.* **1988**, *88*, 7221. (f) Voter, A. F.; Doll, J. D.; Cohen, J. M. *J. Chem. Phys.* **1989**, *90*, 2045. (g) Agrawal, P. M.; Thompson, D. L.; Raff, L. M. *J. Chem. Phys.* **1989**, *91*, 6463. (h) Schranz, H. W.; Raff, L. M.; Thompson, D. L. *Chem. Phys. Lett.* **1990**, *171*, 68; *J. Chem. Phys.* **1991**, *94*, 4219; *Chem. Phys. Lett.* **1991**, *182*, 455. (i) Sewell, T. D.; Schranz, H. W.; Raff, L. M.; Thompson, D. L. *J. Chem. Phys.* **1991**, *95*, 8089.
- (12) Severin, B. C.; Freasier, B. C.; Hamer, N. D.; Jolly, D. L.; Nordholm, S. *Chem. Phys. Lett.* **1978**, *57*, 117.
- (13) Metropolis, N.; Rosenbluth, A. W.; Rosenbluth, M. N.; Teller, A. H.; Teller, E. *J. Chem. Phys.* **1953**, *21*, 1087.
- (14) Behrens, R., Jr.; Bulusu, S. *J. Phys. Chem.* **1992**, *96*, 8877; **1992**, *96*, 8891.
- (15) Wight, C. A.; Botcher, T. R. *J. Am. Chem. Soc.* **1992**, *114*, 8303.
- (16) Botcher, T. R.; Wight, C. A. *J. Phys. Chem.* **1994**, *98*, 5441.